SCIENCE CHINA
Information Sciences

• LETTER •

August 2021, Vol. 64 189303:1–189303:2
https://doi.org/10.1007/s11432-020-3099-6

Ergodic rate analysis for full-duplex NOMA networks with energy harvesting

Bin ZHONG, Long CHEN & Zhijun TANG*

School of Information and Electrical Engineering, Hunan University of Science and Technology, Xiangtan 411201, *China*

Received 3 May 2020/Revised 3 August 2020/Accepted 27 October 2020/Published online 2 June 2021

Citation Zhong B, Chen L, Tang Z J. Ergodic rate analysis for full-duplex NOMA networks with energy harvesting. Sci China Inf Sci, 2021, 64(8): 189303, https://doi.org/10.1007/s11432-020-3099-6

Dear editor,

Non-orthogonal multiple access (NOMA), regarded as a promising technique for substantially increasing the spectral efficiency of wireless networks that comprise massive devices, has exhibited a number of significant performance advantages, including the reduced latency, improved reliability, and the capability of offering a higher sum throughput. Furthermore, a device operating in full-duplex (FD) mode only needs half of the time of a half-duplex (HD) device to complete the same amount of data transmission and reception, because a single channel can be reused to enable a simultaneous transmission and reception [1–3]. Both FD and NOMA technologies have been widely acknowledged as efficient ways for improving the spectrum efficiency of wireless networks [4–6].

In this letter, energy harvesting from the downlink channel of NOMA systems is studied by considering FD mode relays.

System model. A simultaneous wireless information and power transfer (SWIPT) based NOMA network is considered, in which two users can communicate bi-directionally with a source S and the ith user ($U_i, i \in \{1,2\}$). A distance $\|d_i\|$ between S and U_i is considered, where $\|d_1\| < \|d_2\|$. In this system, all the nodes are assumed to be equipped with two antennas and capable of working in FD mode. Without loss of generality, a non-zero residual self-interference (RSI) is assumed in each FD node. Furthermore, the reciprocal channels between the ith user and S (i.e., $h_{S,i}$) are assumed to suffer from independent and identically distributed (i.i.d.) Rayleigh fading. Therefore, $h_{S,i}$ is a normalized cyclic symmetric complex Gaussian variable, i.e., $h_{S,i} \sim \mathcal{CN}(0,1)$. Hence, the channel gain between S and U_i, namely $|h_{S,i}|^2$, follows an i.i.d. exponential distribution with unit mean ($|h_{S,i}|^2 \sim \exp(1)$). Meanwhile, each channel also suffers from additive white Gaussian noise (AWGN). The power of source P_s can be determined by using a power-split parameter α ($0 < \alpha < 1$). In particular, a portion of split power αP_s is used for energy harvesting while the remaining $P_{\rm DL} = (1-\alpha)P_s$ is used for downlink signal transmission. Thus, the superposed downlink signal of the two users is $x = p_1x_1 + p_2x_2$, where p_i and x_i, $i \in \{1,2\}$ denote the transmit power coefficient and downlink signal of the ith user, with $p_1^2 + p_2^2 = 1$, respectively. Finally, the power of each user for uplink transmission is given by

$$P_i^{\rm T} = \frac{P_S\alpha|h_{S,i}|^2}{(\varepsilon + \|d_i\|^\delta)}, \quad (1)$$

where ε is a fixed parameter that ensures a finite harvested energy and path loss, and δ stands for the path loss exponent.

Downlink NOMA signal at the receiver. The downlink NOMA signal received by the ith user ($U_i, i \in 1,2$) can be given as

$$Y_{\rm DL} \rightarrow U_i = \frac{\sqrt{P_{\rm DL}}h_{S,i}}{\sqrt{\varepsilon + \|d_i\|^\delta}}x + \sqrt{P_i^{\rm T}\lambda_i}x_i' + n_i, \quad (2)$$

where x_i' is the uplink signal transmitted by U_i, λ_i denotes the RSI power coefficient for U_i, and $n_i \sim \mathcal{CN}(0,\sigma_i^2)$ stands for the AWGN with zero mean and variance σ_i^2 observed at U_i.

Therefore, the signal-to-interference-plus-noise ratio (SINR) at U_2 for downlink transmission is given by

$$\gamma_{U_2}^{\rm DL} = \frac{\rho_{2,2}|h_{S,2}|^2}{(\rho_{1,2} + \varrho_2\lambda_2)|h_{S,2}|^2 + 1}, \quad (3)$$

where $\rho_{i,j} = \frac{P_{\rm DL}p_i^2}{\sigma_j^2(\varepsilon+\|d_j\|^\delta)}$ and $\varrho_i = \frac{P_S\alpha}{\sigma_i^2(\varepsilon+\|d_i\|^\delta)}, i,j \in \{1,2\}$ denote the power-to-noise ratio for downlink signal and energy transmissions at U_i, respectively.

After performing successive interference cancellation (SIC) in terms of x_2, the received SINR at U_1 for downlink messages x_1 can be given by

$$\gamma_{U_1}^{\rm DL} = \frac{\rho_{1,1}|h_{S,1}|^2}{\varrho_1\lambda_1|h_{S,1}|^2 + 1}. \quad (4)$$

Uplink NOMA signal at the receiver. By exploiting the received power of the ith user's signal differences and implementing SIC at S, we may readily assume that U_1 will no

* Corresponding author (email: zjtang@hnust.edu.cn)

longer interfere with U_2. The uplink NOMA signal received by S is then given by

$$Y_{\rm UP} \rightarrow S = \sum_{i\in\{1,2\}} \frac{\sqrt{P_i^{\rm T}} x_i' h_{S,i}}{\sqrt{\varepsilon + \|d_i\|^\delta}} + \sqrt{P_{\rm DL}\lambda_0} x + n_S, \quad (5)$$

where λ_0 denotes the RSI power coefficient for FD node S, while $n_S \sim \mathcal{CN}(0, \sigma_S^2)$ denotes the AWGN with zero mean and variance σ_S^2 observed at S.

The received SINR at S for uplink messages x_1' can be expressed as

$$\gamma_{S,x_1'}^{\rm UP} = \frac{\vartheta_1 |h_{S,1}|^4}{\vartheta_2 |h_{S,2}|^4 + 1}, \quad (6)$$

where $\vartheta_i = \frac{\alpha P_S}{(\varepsilon + \|d_i\|^\delta)^2 (\lambda_0 P_{\rm DL} + \sigma_S^2)}$.

After performing SIC in terms of x_1', the received SINR at S for uplink messages x_2' can be given by

$$\gamma_{S,x_2'}^{\rm UP} = \vartheta_2 |h_{S,2}|^4. \quad (7)$$

Proposition 1 (Downlink ergodic data rate)**.** The downlink ergodic data rate for the FD-SWIPT based transmission model is given by

$$\begin{aligned} R^{\rm DL} = & \frac{1}{\ln 2}\left[\exp\left(\frac{1}{\varrho_1\lambda_1 + \rho_{1,1}}\right) E_1\left(\frac{1}{\varrho_1\lambda_1 + \rho_{1,1}}\right)\right. \\ & \left. - \exp\left(\frac{1}{\varrho_1\lambda_1}\right) E_1\left(\frac{1}{\varrho_1\lambda_1}\right)\right] \\ & + \frac{1}{\ln 2}\left[\exp\left(\frac{1}{\rho_{1,2} + \varrho_2\lambda_2 + \rho_{2,2}}\right)\right. \\ & \times E_1\left(\frac{1}{\rho_{1,2} + \varrho_2\lambda_2 + \rho_{2,2}}\right) \\ & \left. - \exp\left(\frac{1}{\rho_{1,2} + \varrho_2\lambda_2}\right) E_1\left(\frac{1}{\rho_{1,2} + \varrho_2\lambda_2}\right)\right], \end{aligned} \quad (8)$$

where $E_1(x) = \int_x^{+\infty} \frac{{\rm e}^{-t}}{t} {\rm d}t = -\mathtt{Ei}(-x)$, with $\mathtt{Ei}(\cdot)$ denoting the exponential integral function [7, Eq.8.211.1].

Proof. The proof is given in Appendix A.

Proposition 2 (Uplink ergodic data rate)**.** The uplink ergodic data rate for the FD-SWIPT based transmission model is given by

$$\begin{aligned} R^{\rm UP} = & \frac{\pi}{K\ln 2} \sum_{k=1}^{K} a_k \left[-\sin(b_k)\,\mathtt{si}(b_k) - \cos(b_k)\,\mathtt{ci}(b_k)\right] \\ & + \frac{2}{\ln 2}\left[-\sin\left(\frac{1}{\sqrt{\vartheta_2}}\right) \mathtt{si}\left(\frac{1}{\sqrt{\vartheta_2}}\right)\right. \\ & \left. - \cos\left(\frac{1}{\sqrt{\vartheta_2}}\right) \mathtt{ci}\left(\frac{1}{\sqrt{\vartheta_2}}\right)\right], \end{aligned} \quad (9)$$

where $\mathtt{si}(x) = -\int_x^{+\infty} \frac{\sin(t)}{t} {\rm d}t$ and $\mathtt{ci}(x) = -\int_x^{+\infty} \frac{\cos(t)}{t} {\rm d}t$ denote the sine and cosine integral functions [7, Eq.8.230.1, Eq.8.230.2], respectively.

Proof. The proof is given in Appendix B.

Numerical results. Figure 1 illustrates the downlink and uplink data rates versus the signal-to-noise ratio (SNR) (i.e., P_S/σ^2) with variant α. It is shown that the uplink data rate can be improved by providing more power to the energy harvesting users. Furthermore, a fundamental tradeoff between uplink and downlink data rates is observed: the uplink data rate can be obtained at the cost of sacrificing the downlink data rate, as shown in Figure 1. Anyway, the ratio of the uplink rate to the downlink rate can be adaptively adjusted by optimizing α according to each user's requirement, thus demonstrating the benefits of employing SWIPT.

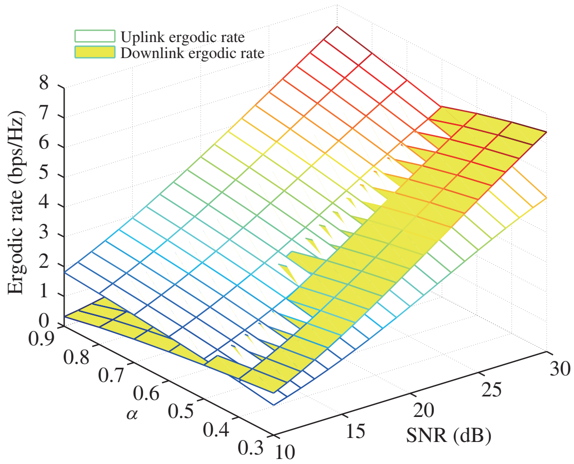

Figure 1 (Color online) Ergodic data rates vs. α and SNR.

Conclusion. The ergodic data rate in SWIPT-aided NOMA-based wireless networks was studied by considering FD mode in the nodes. The closed-form expressions of data rates for both downlink and uplink transmissions were derived, following which the validity of the theoretical expressions was verified by using simulations. Furthermore, it was illustrated that some critical parameters (e.g., the average SNR of each link, the power-split parameter, etc.) may substantially impact the uplink/downlink data rates.

Acknowledgements This work was supported by National Natural Science Foundation of China (Grant Nos. 62071035, 61905074, 61875054), Hunan Provincial Natural Science Foundation of China (Grant Nos. 2020JJ4318, 2019JJ50170), and Research Foundation of Education Department of Hunan Province (Grant No. 18C0326).

Supporting information Appendixes A and B. The supporting information is available online at info.scichina.com and link.springer.com. The supporting materials are published as submitted, without typesetting or editing. The responsibility for scientific accuracy and content remains entirely with the authors.

References

1 Lu Z Y, Sun L L, Zhang S, et al. Optimal power allocation for secure directional modulation networks with a full-duplex UAV user. Sci China Inf Sci, 2019, 62: 080304
2 Luo S X, Zhang Z S, Wang S, et al. Network for hypersonic UCAV swarms. Sci China Inf Sci, 2020, 63: 140311
3 Zhong B, Zhang Z, Chai X, et al. Performance analysis for opportunistic full-duplex relay selection in underlay cognitive networks. IEEE Trans Veh Technol, 2015, 64: 4905–4910
4 Zhong B, Zhang Z. Secure full-duplex two-way relaying networks with optimal relay selection. IEEE Commun Lett, 2017, 21: 1123–1126
5 Zhong B, Zhang Z. Opportunistic two-way full-duplex relay selection in underlay cognitive networks. IEEE Syst J, 2018, 12: 725–734
6 Zeng Q, Zheng Y, Zhong B, et al. Minimum transmission protocol for full-duplex systems with energy harvesting. IEEE Commun Lett, 2019, 23: 382–385
7 Gradshteyn I S, Ryzhik I M. Table of Integrals, Series, and Products. 7th ed. New York: Academic, 2007